Supporting Information

Kaneuchi et al. 10.1073/pnas.1420589112

SI Materials and Methods

Fly Strains. *attP*(ZH-51D), P{*y*[+t7.7]=CaryIP}*su(Hw)attP5*, P{*y*[+t7.7]=CaryIP}*su(Hw)attP2*, *matα4-GAL-VP16*, $itpr^{ka901}$, $itpr^{ug3}$, *hs*FLP[1], and shRNA fly stocks (1) were obtained from the Bloomington Stock Center. For generation of germline clones, neoFRT(82B) PBac{SAstopDsRed}LL02136 (2), which was crossed to *itpr* mutants to generate the recombinant chromosomes with FRT, and neoFRT(82B) $ovo^{D1\text{-}18}$ were obtained from the *Drosophila* Genetic Resource Center (Kyoto, Japan).

DNA Constructs and Transgenic Flies. *pUASp*-GFP-aequorin-*attB* (3) used in the transgenic flies in Fig. S1*B* and Fig. S3 and in Movies S4 and S6 was constructed as follows. The appropriate EcoRV and PstI fragment of *pUASp* and the EcoRI and XhoI fragment that contains the entire ORF for GFP–aequorin from pGGA2 (4) were cloned into a modified version of pUAST-*attB* (5). The construct was integrated into the *attP* site at M{3xP3-RFP.*attP*}ZH-51D (5) in the *y w* genetic background, and transgenic lines were stabilized by standard procedures.

Germline Clonal Analyses. Germline clones of $itpr^{ka901}$, a functionally null allele, and $itpr^{ug3}$, an altered sensitivity allele of *Itp-r83A*/IP3R (6, 7), were produced by the flippase-dominant female sterile technique (8). *matα4-GAL-VP16*, *UASp-GFP-GCaMP3*; neoFRT(82B), $itpr^{ka901}$/*TM6B*, *Tb* or *matα4-GAL-VP16*, *UASp-GFP-GCaMP3*; neoFRT (82B), $itpr^{ug3}$/*TM6B*, *Tb*; or *matα4-GAL-VP16*, *UASp-GFP-GCaMP3*/+; neoFRT(82B)/*TM6B*, *Tb* (control) females were crossed to hsFLP[1]/Y; neoFRT(82B), $ovo^{D1\text{-}18}$/*TM3*, *Sb* males. Third instar larvae were heat-treated twice for 2 h at 37 °C, and the eclosed Tb^+ Sb^+ females were used for the experiment. As noted in the text, the germline clone eggs obtained in these experiments were fragile, but it is not certain that that was due to the *itpr* mutation, as control eggs in this genetic background also showed fragility.

Bioluminescence Microscopy. GFP–aequorin-based bioluminescence and BRET signal was imaged using a LV200 bioluminescence imaging system (Olympus). Oocytes containing GFP–aequorin were dissected from transgenic females (*matα4-GAL-VP16>UASp-GFP-aequorin*) and individually incubated with 50 μL of isotonic HL3 saline (9) containing 2 mM Ca^{2+} and 100 μM coelenterazine (JNC) in a glass-bottomed dish (MAT-TEK) for 3–5 h at room temperature. The dish containing the oocytes was placed in the imaging system, and 100 μL of ddH_2O was added to induce activation by hypotonic stimulation. Images were captured at the rate of one frame per second.

1. Ni JQ, et al. (2008) Vector and parameters for targeted transgenic RNA interference in *Drosophila melanogaster*. *Nat Methods* 5(1):49–51.
2. Schuldiner O, et al. (2008) piggyBac-based mosaic screen identifies a postmitotic function for cohesin in regulating developmental axon pruning. *Dev Cell* 14(2):227–238.
3. Baubet V, et al. (2000) Chimeric green fluorescent protein-aequorin as bioluminescent Ca2+ reporters at the single-cell level. *Proc Natl Acad Sci USA* 97(13):7260–7265.
4. Martin JR, Rogers KL, Chagneau C, Brûlet P (2007) In vivo bioluminescence imaging of Ca signalling in the brain of *Drosophila*. *PLoS ONE* 2(3):e275.
5. Bischof J, Maeda RK, Hediger M, Karch F, Basler K (2007) An optimized transgenesis system for *Drosophila* using germ-line-specific phiC31 integrases. *Proc Natl Acad Sci USA* 104(9):3312–3317.
6. Joshi R, Venkatesh K, Srinivas R, Nair S, Hasan G (2004) Genetic dissection of itpr gene function reveals a vital requirement in aminergic cells of *Drosophila* larvae. *Genetics* 166(1):225–236.
7. Srikanth S, et al. (2004) Functional properties of the *Drosophila melanogaster* inositol 1,4,5-trisphosphate receptor mutants. *Biophys J* 86(6):3634–3646.
8. Chou TB, Perrimon N (1996) The autosomal FLP-DFS technique for generating germline mosaics in *Drosophila melanogaster*. *Genetics* 144(4):1673–1679.
9. Stewart BA, Atwood HL, Renger JJ, Wang J, Wu CF (1994) Improved stability of *Drosophila* larval neuromuscular preparations in haemolymph-like physiological solutions. *J Comp Physiol A Neuroethol Sens Neural Behav Physiol* 175(2):179–191.

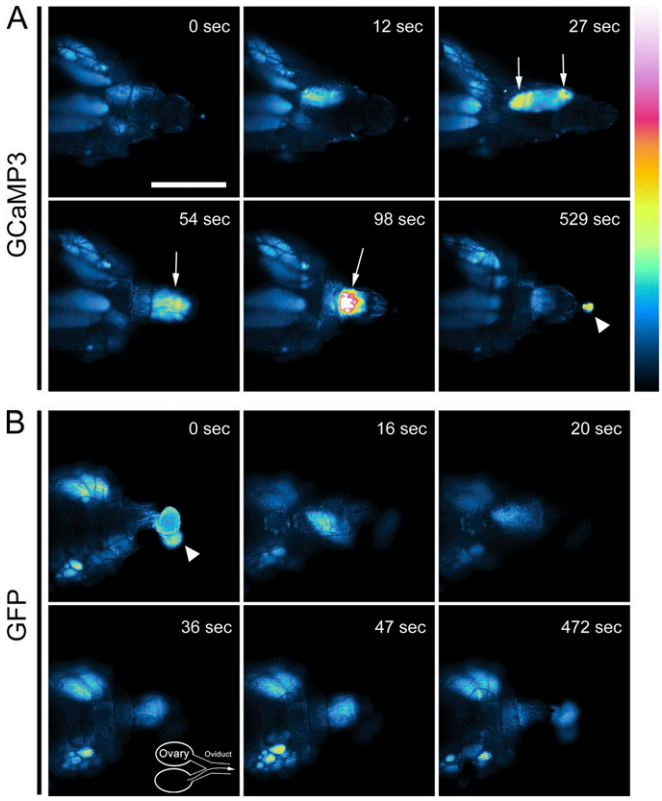

Fig. S1. Ca^{2+} rise in oocytes during ovulation in vivo. We imaged the ovulation process under a confocal laser-scanning fluorescence microscope (Nikon C1si) for a more detailed view; ventral views of the females are shown; anterior is to the left. (*A*) Shows the rise in calcium as an egg is ovulated; these are still frames from Movie S3. In vivo Ca^{2+} imaging was performed on transgenic female flies expressing GCaMP3 in their oocytes. *B*, which shows still frames from Movie S4, is the control. The oocytes imaged here were in transgenic *matα4-GAL-VP16>UASp*-GFP–aequorin females. The GFP–aequorin expressed in the oocytes of these females does not fluoresce in response to calcium unless coelenterazine is included to cause aequorin luminescence (which would then induce GFP fluorescence by BRET). No coelenterazine was present in these experiments. Thus, the fluorescence of their GFP–aequorin is insensitive to calcium levels and serves as negative control for basal GFP fluorescence. An intense fluorescence signal is induced in oocytes as they are ovulated in females expressing GCaMP3 but not in oocytes of females that expressed GFP–aequorin. Arrows indicate fluorescence signals corresponding to descending eggs. Ovaries are weakly fluorescent, and there is strong auto-fluorescence in the feces (arrowheads). The fluorescent signal of an egg increased as it moved downward (toward the posterior end of the abdomen), and the intensity was at maximum when the oocytes descended to a certain position, most likely the uterus (98 s). The time after release from the ovary is indicated in each panel. Fluorescence intensities are presented using a false-color scale on the right side. (Scale bar, 500 μm.) There is a schematic for orientation in *B*, *Lower Left*. This figure typifies what we saw in >20 ovulating oocytes. Peristaltic motions inside the female made the image occasionally go out of sharpest focus.

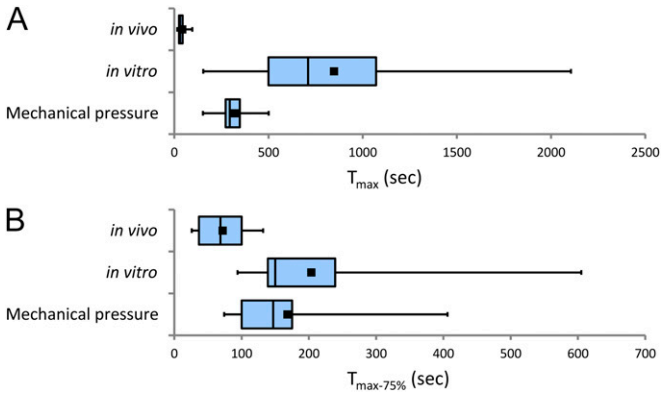

Fig. S2. Quantitative analysis of Ca^{2+} fluorescence intensity (delta F/F0). (*A*) T_{max} represents the time required to reach the maximum intensity from the time 0 at which the fluorescence intensity started to increase. The increase is fastest in vivo. Mechanical pressure in vitro accelerates the in vitro rate. (*B*) T_{max}-75 represents the time required to return to 75% of the maximum intensity from the time of peak (T_{max}). n = 10 in vivo, 14 in vitro, and 8 mechanical pressure.

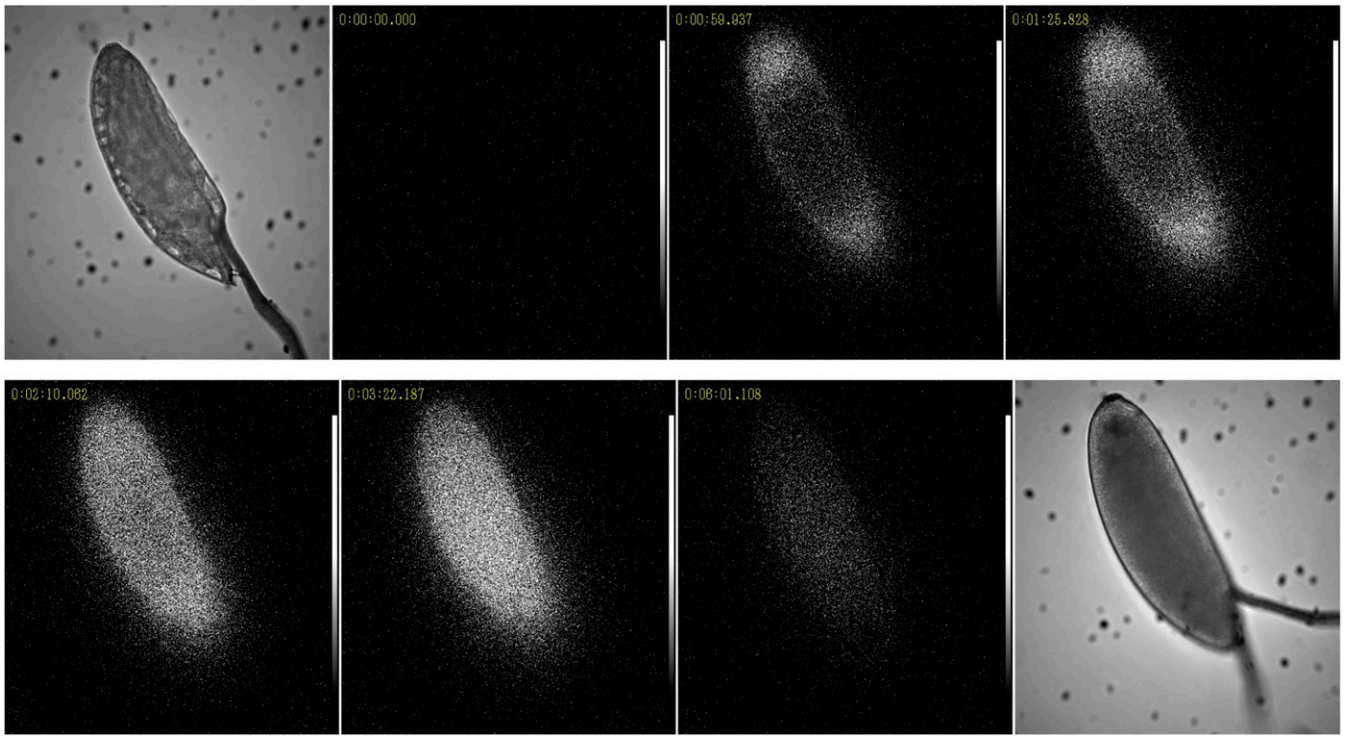

Fig. S3. Ca^{2+} influx visualized by bioluminescence with GFP–aequorin. Oocytes were dissected from transgenic female flies expressing GFP–aequorin (3) in their oocytes (*matα4-GAL-VP16>UASp-GFP-aequorin*) in HL3 buffer (9) and incubated with 50 mM coelenterazine and 2 mM $CaCl_2$ in HL3 buffer for 3 h. HL3 was used instead of IB because uptake of the substrate coelenterazine was more efficient in HL3. In vitro activation was induced by diluting HL3 with water. Ca^{2+} imaging was performed using an Olympus Bioluminescence Imaging System LV200 to visualize the calcium-stimulated signal emitted from GFP as a result of BRET from the aequorin moiety. Panels are from Movie S6. The pattern of the observed signal was consistent with the calcium wave observed with GCaMP3 oocytes (Figs. 1 and 2 and Fig. S1; Movies S1, S3, S5, and S7). *Upper Left* and *Lower Right* are brightfields of the panels to their right and left, respectively.

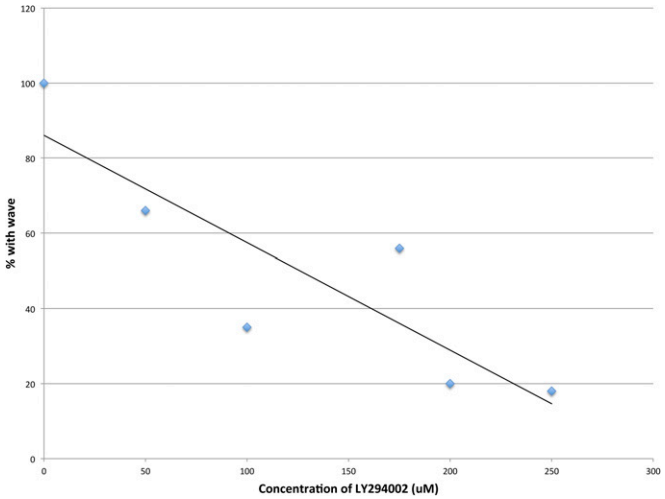

Fig. S4. LY294002 inhibits the calcium rise. GCaMP3-containing oocytes were incubated in a range of concentrations of LY294002 (or control), and the calcium wave was imaged. Methods and analysis were as in Fig. 3. The percentage of oocytes that showed a calcium wave is graphed. LY204002 at all concentrations inhibited the calcium rise (50 μM LY294002, $P = 0.0230$; 100 μM LY294002, $P < 0.0001$; 175 μM LY294002, $P = 0.0014$; 200 μM LY294002, $P < 0.0001$; 250 μM LY294002, $P < 0.0001$), and the effect was dose-responsive. $n = 9$–17 tested per concentration.

Table S1. Effects of inhibitors on acquisition of bleach resistance (egg activation) and calcium wave

Drug	Function	Method	Activation
BAPTA	Ca^{2+} chelator	Bleach assay	–
	Chelate Ca^{2+} in buffer to <50 nM	GCaMP3 microscopy	–
$GdCl_3$	Blocks stretch-activated channels	100 μM, bleach assay	–
		100–400 μM, GCaMP microscopy	–
		10 μM, GCaMP microscopy	+
Ruthenium red	Blocks ryanodine receptor	10 μM, bleach assay	+
		10–20 μM, GCaMP3 microscopy	+

Bleach assay was carried out as in ref. 1. Results are summarized from ref. 2 and Fig. 3. For bleach assay: +, eggs become resistant to lyse in bleach (activated) after incubation in AB with inhibitor; –, eggs lyse in bleach (fail to activate) after incubation in AB with inhibitor. For microscopy: +, a calcium rise is seen upon incubation in AB with inhibitor; –, no calcium rise is seen upon incubation in AB with inhibitor.

1. Heifetz Y, Yu J, Wolfner MF (2001) Ovulation triggers activation of *Drosophila* oocytes. *Dev Biol* 243(2):426–424.
2. Horner VL, Wolfner MF (2008) Mechanical stimulation by osmotic and hydrostatic pressure activates *Drosophila* oocytes in vitro in a calcium-dependent manner. *Dev Biol* 316(1):100–109.

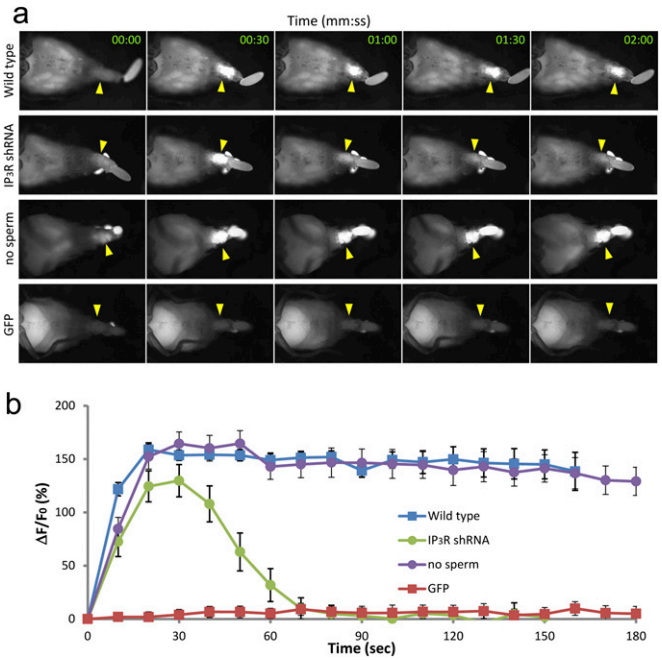

Movie S1. In vivo imaging at dissection scope resolution of Ca^{2+} flux in activating oocytes from transgenic flies expressing GCaMP3 in their oocytes. See text and the legend to Fig. 1*A* for details.

Movie S1

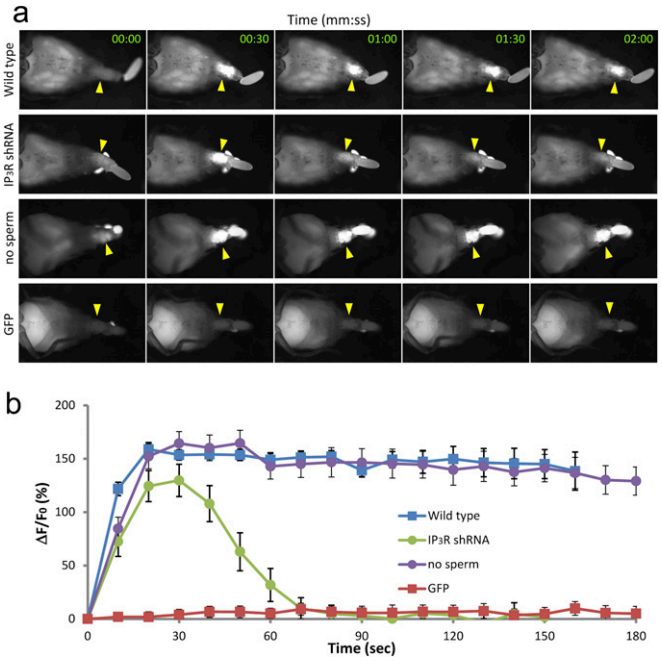

Movie S2. In vivo imaging at dissection scope resolution of activating oocytes from control transgenic flies expressing GFP in their oocytes. See text and the legend to Fig. 1*A* for details.

Movie S2

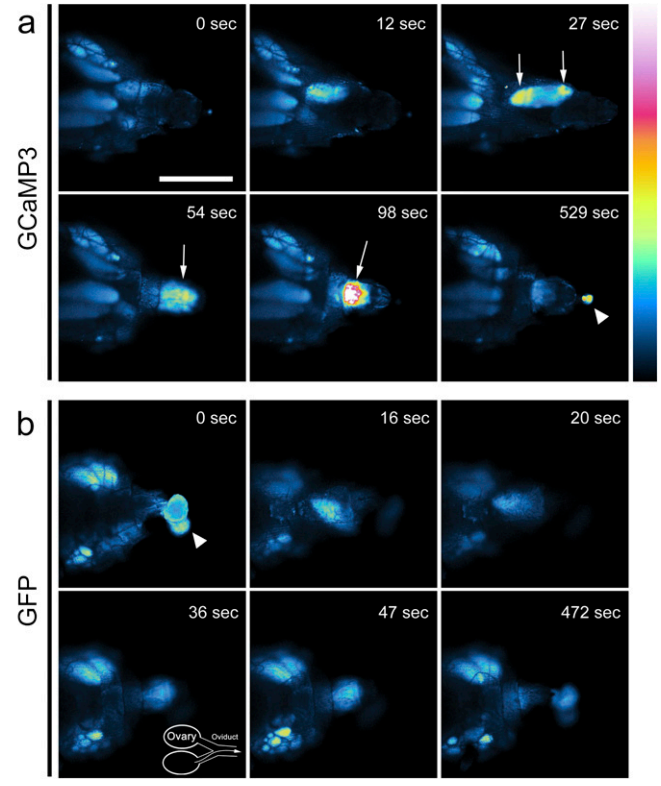

Movie S3. In vivo imaging at high magnification of Ca^{2+} flux in activating oocytes from transgenic flies expressing GCaMP3 in their oocytes. See text and the legend to Fig. S1 for details.

Movie S3

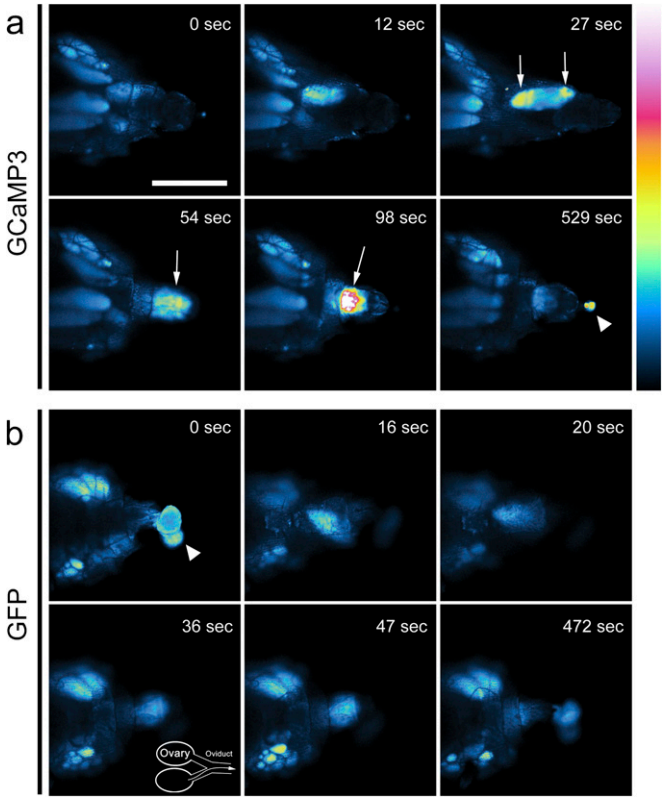

Movie S4. In vivo imaging at high magnification of activating oocytes from transgenic control flies, which express GFP–aequorin in their oocytes. This imaging was in the absence of coelenterazine, so any fluorescence from the GFP is independent of calcium. See text and the legend to Fig. S1 for details.

Movie S4

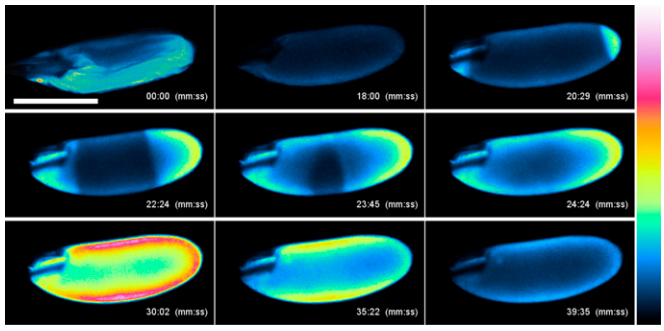

Movie S5. Ca^{2+} flux in GCaMP-containing oocytes activated in vitro. See text and the legend to Fig. 2 for details. We believe that the brief "fluttering" in the signal that occurs occasionally in this movie is a consequence of transient differences in local Ca^{2+} flux, perhaps due to small fluctuations of Ca^{2+} concentration in the solution around the oocyte.

Movie S5

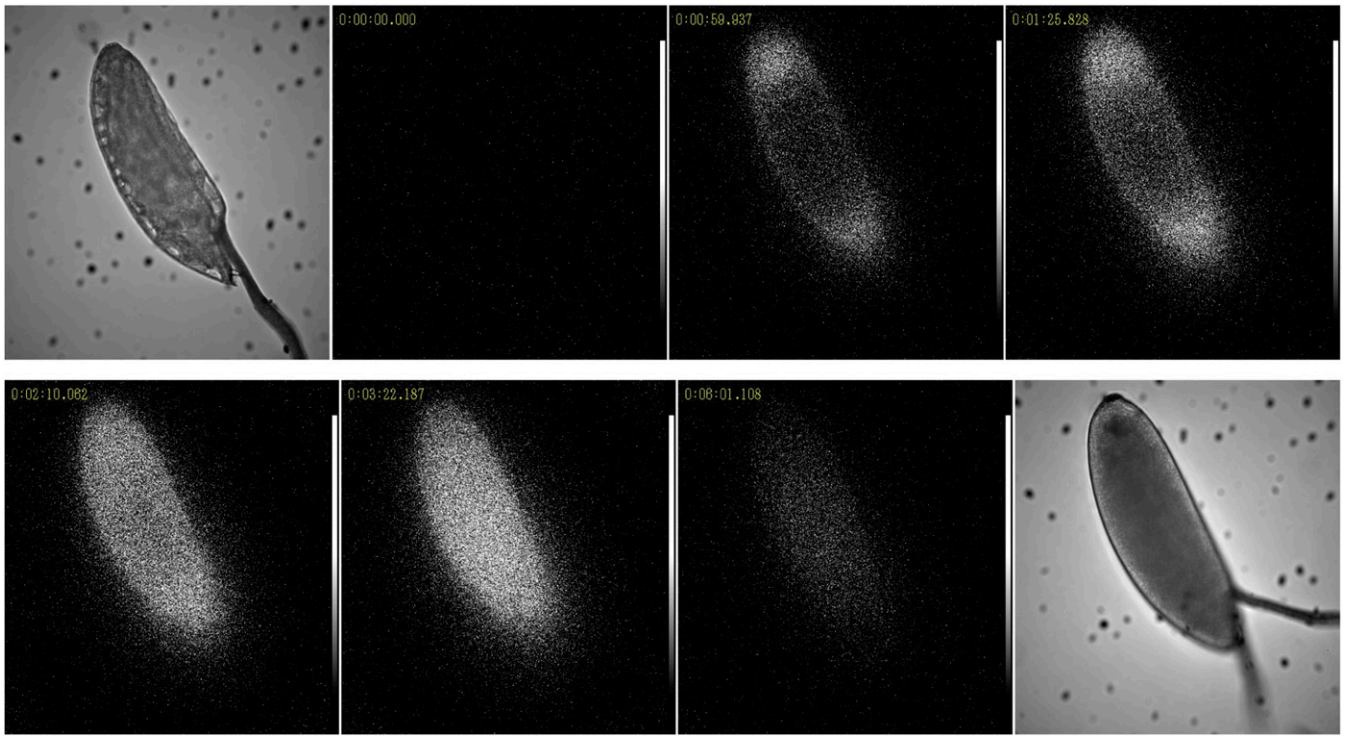

Movie S6. Ca^{2+} flux in GFP–aequorin oocytes activated in vitro in the presence of coelenterazine as visualized by bioluminescence. See text and legend to Fig. S3 for details.

Movie S6

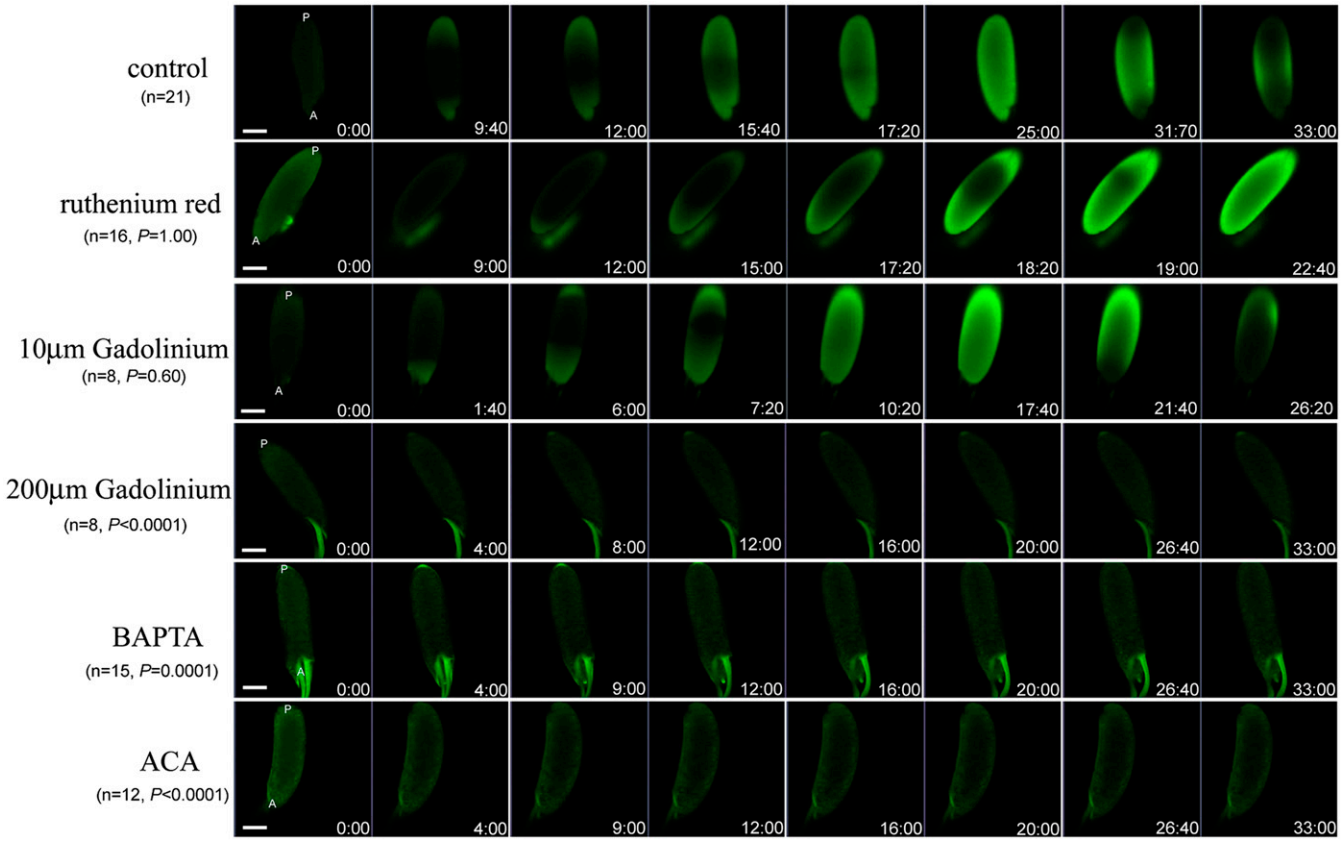

Movie S7. Oocyte swelling precedes Ca^{2+} rise. The oocyte shown was dissected from a *nos-GCaMP* female and incubated in vitro under control conditions. See text and legend to Fig. 3 for details.

Movie S7

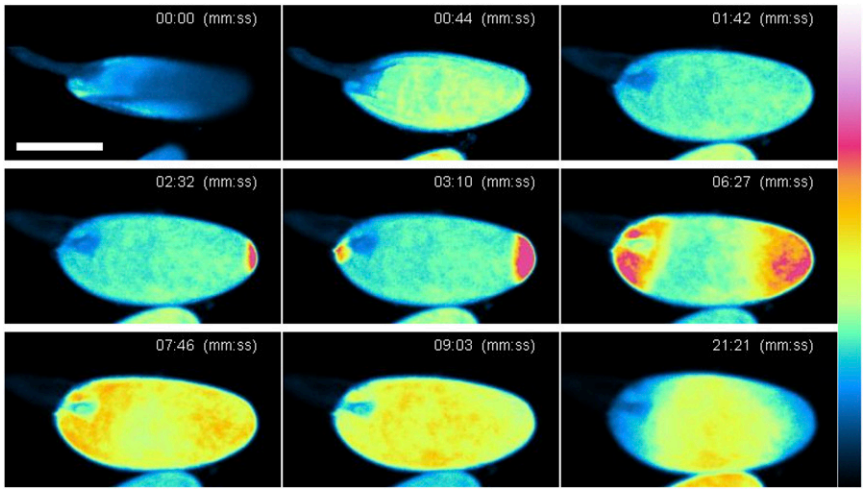

Movie S8. Ca^{2+} flux in GCaMP-containing oocytes upon mechanical stimulation. See text and legend to Fig. 4 for details.

Movie S8

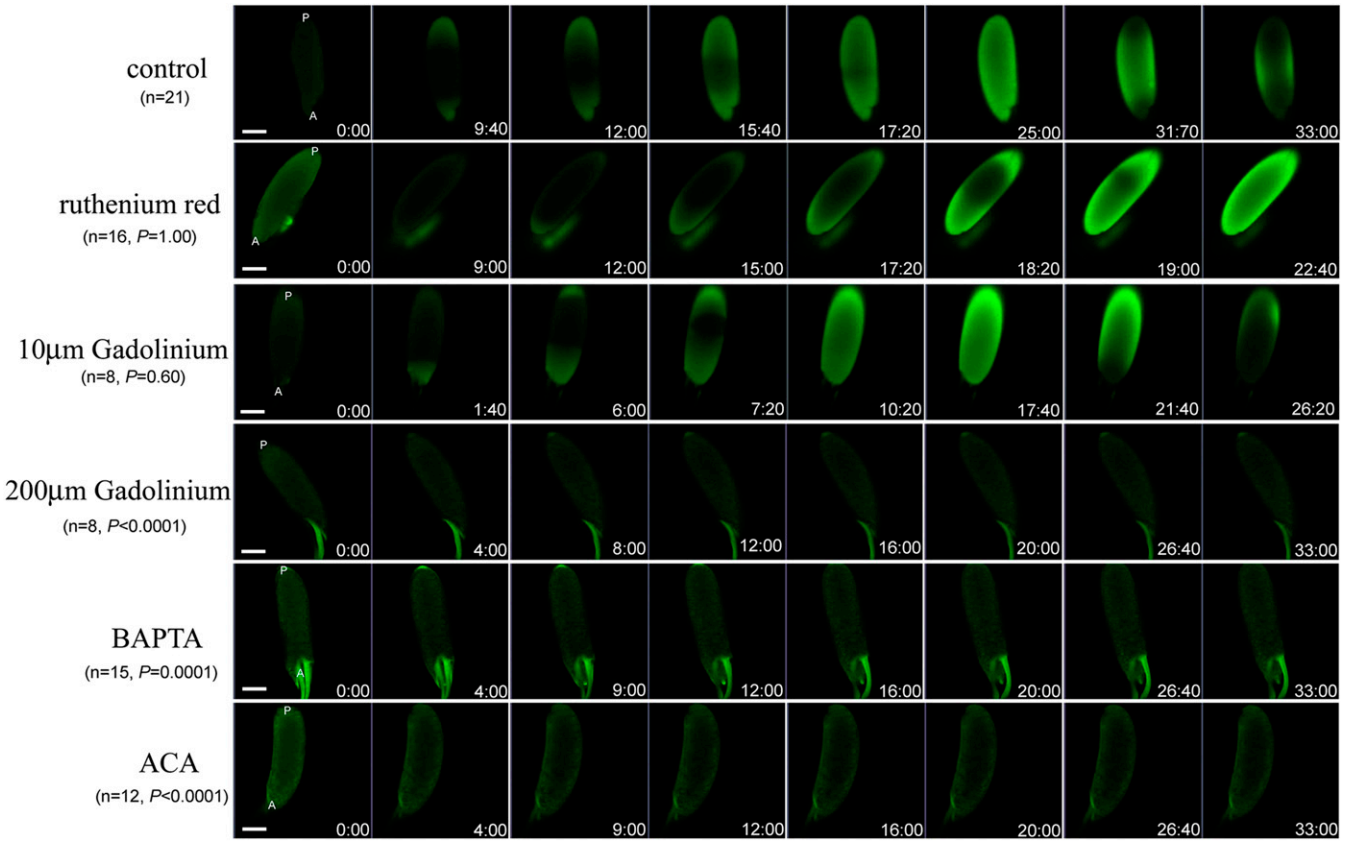

Movie S9. $GdCl_3$ (10 µM) does not prevent the calcium wave. The oocyte shown was dissected from a *nos-GCaMP* female, and incubated in vitro. See text and legend to Fig. 3 for details.

Movie S9

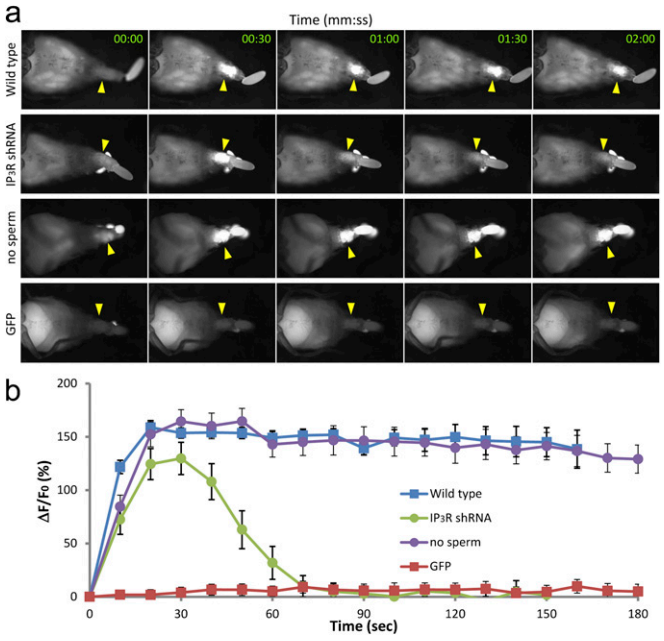

Movie S10. In vivo imaging at dissection scope resolution of Ca^{2+} flux in activating oocytes from transgenic flies expressing GCaMP3, but also knocked down for IP3R, in their oocytes. See text, and the legend to Fig. 1*A*, for details.

Movie S10

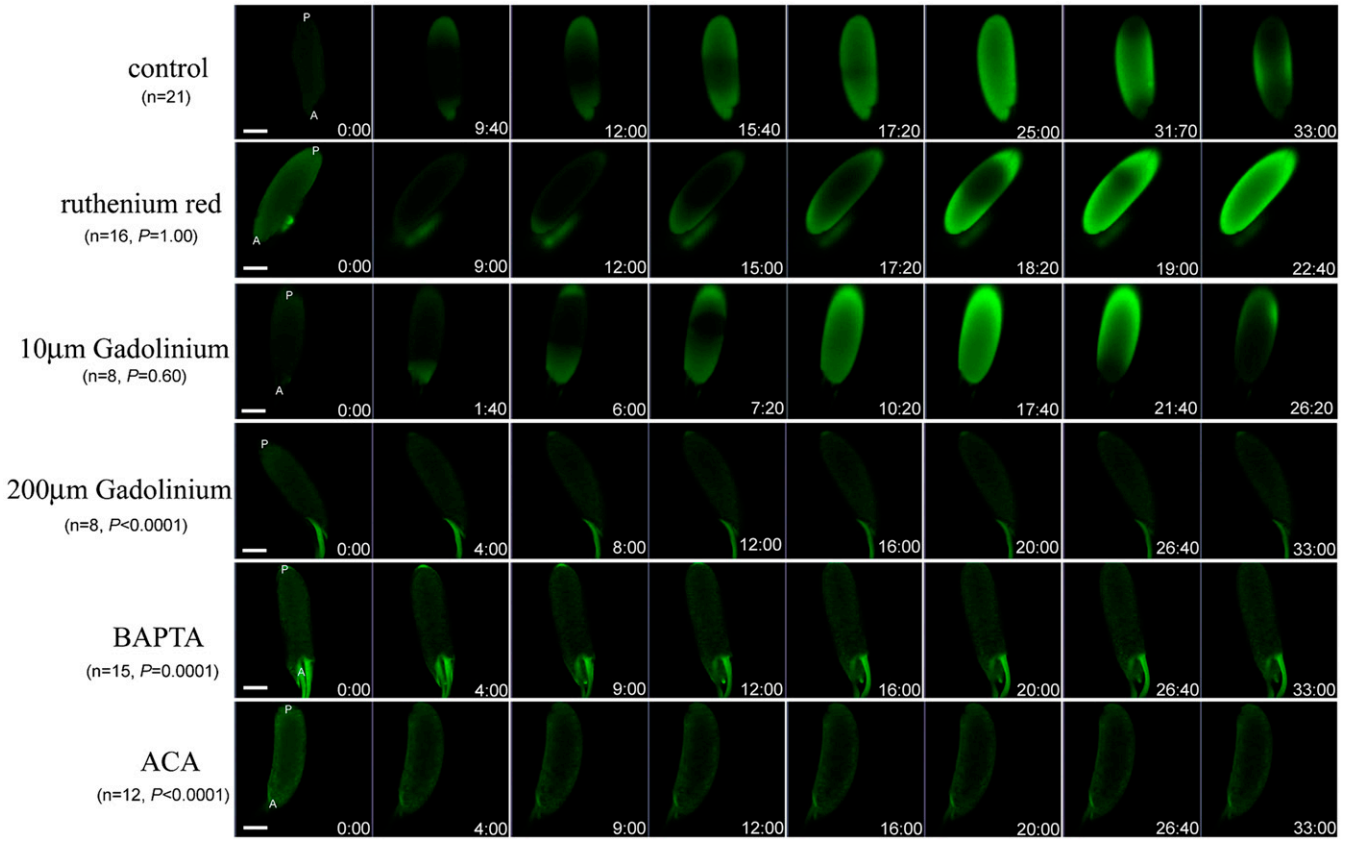

Movie S11. Ruthenium red does not prevent the calcium wave. The oocyte shown was dissected from a *nos-GCaMP* female, and incubated in vitro. See text and legend to Fig. 3 for details.

Movie S11